Biomaterials Advances 153 (2023) 213576

Contents lists available at ScienceDirect

Biomaterials Advances

journal homepage: www.journals.elsevier.com/materials-science-and-engineering-c

Primary human hepatocytes-laden scaffolds for the treatment of acute liver failure

Julio Rodriguez-Fernandez [a], Emma Garcia-Legler [a], Estela Villanueva-Badenas [b,c], M. Teresa Donato [b,c,d], José Luis Gomez-Ribelles [a,e], Manuel Salmeron-Sanchez [a,e,f], Gloria Gallego-Ferrer [a,e,*], Laia Tolosa [b,e,**]

[a] Center for Biomaterials and Tissue Engineering (CBIT), Universitat Politècnica de València, Valencia 46022, Spain
[b] Experimental Hepatology Unit, Health Research Institute La Fe (IISLAFE), Valencia 46026, Spain
[c] Departamento de Bioquímica y Biología Molecular, Facultad de Medicina, Universidad de Valencia, Valencia 46010, Spain
[d] Centro de Investigación Biomédica en Red de Enfermedades Hepáticas y Digestivas (CIBERehd), Instituto de Salud Carlos III, Madrid, Spain
[e] Biomedical Research Networking Center on Bioengineering, Biomaterials and Nanomedicine (CIBER-BBN), Valencia, Spain
[f] Centre for the Cellular Microenvironment, Division of Biomedical Engineering, School of Engineering, University of Glasgow, G12 8LT Glasgow, United Kingdom

ARTICLE INFO

Keywords:
Gelatin
Hyaluronic acid
Hydrogels
Scaffolds
Liver cell therapy
Acute liver failure

ABSTRACT

Cell-based liver therapies based on retrieving and steadying failed metabolic function(s) for acute and chronic diseases could be a valuable substitute for liver transplants, even though they are limited by the low engraftment capability and reduced functional quality of primary human hepatocytes (PHH). In this paper we propose the use of gelatin-hyaluronic acid (Gel-HA) scaffolds seeded with PHH for the treatment of liver failure. We first optimized the composition using Gel-HA hydrogels, looking for the mechanical properties closer to the human liver and determining HepG2 cells functionality. Gel-HA scaffolds with interconnected porosity (pore size 102 μm) were prepared and used for PHH culture and evaluation of key hepatic functions. PHH cultured in Gel-HA scaffolds exhibited increased albumin and urea secretion and metabolic capacity (CYP and UGT activity levels) compared to standard monolayer cultures. The transplant of the scaffold containing PHH led to an improvement in liver function (transaminase levels, necrosis) and ameliorated damage in a mouse model of acetaminophen (APAP)-induced liver failure. The study provided a mechanistic understanding of APAP-induced liver injury and the impact of transplantation by analyzing cytokine production and oxidative stress induction to find suitable biomarkers of cell therapy effectiveness.

1. Introduction

Liver disease causes around 2 million deaths annually [1] and represents a serious health and economic problem. The unique curative treatment for end-stage liver disease is a transplant, but the suitable donor organ availability does not satisfy the clinical need [2]. In Europe, >7000 liver transplants are carried out every year, and around 50 % of the patients have to wait 3 months or more for a suitable organ [3]. Although different surgical techniques have emerged to overwhelm donor scarcity, other alternative treatments such as cell transplantation have appeared for correcting genetic disorders that result in metabolically deficient states for acute liver failure (ALF) or end-stage liver disease patients, or even for preserving liver function in patients not eligible for liver transplants for different reasons (*i.e.* cardiovascular issues, advanced age, or other underlying diseases) [4–6]. Cell transplantation would reduce the need for invasive surgery and the morbidities associated with lifelong immunosuppression, acting as an alternative treatment or as a bridge to organ transplants.

Primary human hepatocytes (PHH) are the gold-standard for both cell-based experiments and clinical application [7–9]. Although they retain key hepatic-specific functions *in vitro* [10], the use of PHH is hampered by the growing lack of suitable donor organs for hepatocyte

* Correspondence to: G. Gallego-Ferrer, Center for Biomaterials and Tissue Engineering (CBIT), Universitat Politècnica de València, Camino de vera s/n, 46022 Valencia, Spain.
** Correspondence to: L. Tolosa, Unidad de Hepatología Experimental, Torre A. Instituto Investigación Sanitaria La Fe, Av Fernando Abril Martorell 106, 46026 Valencia, Spain.
E-mail addresses: ggallego@ter.upv.es (G. Gallego-Ferrer), laiatolosa@hotmail.com, laia_tolosa@iislafe.es (L. Tolosa).

https://doi.org/10.1016/j.bioadv.2023.213576
Received 28 February 2023; Received in revised form 29 June 2023; Accepted 30 July 2023
Available online 5 August 2023

isolation as well as by the deficient quality, progressive loss of functionality (especially phase I and phase II enzyme activities) [11–13] and a pronounced sensitivity to freezing and thawing processes [5,14]. As cells *in vivo* have a three-dimensional (3D) morphology and organization, there is now intense pressure for *in vitro* models that can maintain their morphology and a stable phenotype in culture. PHH 3D models have been shown to extend viability and increase long-term functionality [15]. 3D cultures comprise different systems, from spheroids to 3D scaffolds and also more innovative systems using microfluidics. However, although several 3D approaches have been described for *in vitro* applications such as drug screening or disease modeling for clinical utilization, the improvement of functionality, biodegradability and biocompatibility, as well as adequate evaluation of the *in vivo* effects should still be thoroughly explored.

The ability of donor cells to access the liver and survive long enough to exert a beneficial therapeutic effect could be a significant obstacle to successful transplantation. Although cells integrate in the liver parenchyma after accessing through the sinusoids [2,16], they need appropriate signals as well as an advantage over host cells to significantly repopulate the liver [17]. In this regard, extrahepatic liver cell therapy, which provides functional assistance to the injured liver and allows vascularization, has recently been proposed as a delivery and retention method. Dhawan *et al.* described a first-in-human study analyzing the outcome of the peritoneal administration of microencapsulated PHH in pediatric patients with ALF. They used cryopreserved PHH encapsulated in alginate microbeads and obtained promising results, since four of the eight patients treated avoided a liver transplant [18]. ALF in children presents high mortality and morbidity rates, and although the study by Dhawan *et al.* is only a case series and it will be necessary to obtain data from more patients, the biochemical and clinical improvements seen after transplantation confirm the previous promising results in animals [19]. However, the safety of the procedure remains uncertain since even though alginate is biocompatible it is non-biodegradable in mammals [20] and the long-term effects have not been studied [21]. Also, as alginate is a biologically inert material, it offers limited support to biological functions such as cell attachment and growth. The liver extracellular matrix (ECM) plays a relevant role in cell behavior, enabling cell-cell and cell-ECM interactions, as well as promoting migration, proliferation, and differentiation [22]. Modifications in the composition of liver ECM are related to the development of diseases such as fibrosis or cancer [23,24]. Liver ECM contains a considerable number of components, including proteins such as collagen type I, II and IV, glycoproteins such as laminin and fibronectin and glycosaminoglycans such as hyaluronic acid (HA). In this sense, the use of decellularized liver scaffolds [25,26], natural and synthetic hydrogels [18,19,27,28] and cell sheets [29] have been proposed in liver cell therapy to improve or maintain liver functions and to act as a delivery method.

In this study we demonstrated the use of gelatin-hyaluronic acid (Gel-HA) hydrogels and scaffolds for liver cell transplantation. HA is the main component of the perisinusoidal space and has been proposed as a biocompatible material either alone or in combination with other materials such as collagen or laminin for liver regenerative medicine purposes [30,31]. On the other hand, gelatin is a natural component of the ECM derived from denatured collagen type I and is a biodegradable and inexpensive material that has also been proposed for hepatocyte culture [32]. Although gelatin is a highly promising material, it lacks mechanical properties. Improved mechanical properties were obtained by mixing with HA, with excellent results in other tissue engineering applications [33,34], which opens the way for the 3D culture of PHH. In addition, we show that Gel-HA scaffolds seeded with PHH have therapeutic effects on the established mouse model of acetaminophen-induced ALF. Histopathological examinations and serum biochemical analyses provided a mechanistic understanding of the therapeutic effects of this liver cell therapy.

2. Material and methods

2.1. Material

The reagents for the cell culture, including the complements, were obtained from GIBCO (ThermoFisher, Madrid, Spain) and other chemicals were purchased from Sigma Aldrich (Madrid, Spain). Cell Banker medium was purchased from Amsbio (AMS Biotechnology, Abingdon, UK).

2.2. Gel-HA hydrogels synthesis

Pristine materials, gelatin (from porcine skin, gel strength 300, type A) and hyaluronic acid (sodium salt from *Streptococcus equi*) were modified by grafting tyramine molecules able to enzymatically react to form *in situ* crosslinking hydrogels, as previously described [35].

Hydrogel mixtures of Gel-HA were obtained by mixing different proportions of 2 % wt/vol Gel-HA tyramine solutions (100–0, 80–20, 50–50, 20–80 and 0–100 vol/vol) in F12 medium at 37 °C. Gel solution was prepared at 37 °C for 30 min. HA solution was prepared at 4 °C for 24 h and heated to 37 °C for hydrogel preparation. Every hydrogel was formed by mixing 80 vol% of the Gel-HA mixtures in different proportions, 10 vol% of 12.5 U/mL HRP (1.25 U/mL in the final volume) and 20 mM H_2O_2 (2 mM in the final volume). The crosslinking time of the different hydrogels was measured by a rheometer.

2.3. Gel-HA scaffold preparation

Tyramine derivatives of Gel and HA were dissolved in Calcium Free Krebs Ringer Buffer (CFKRB) at 2 % wt/vol. The Gel-HA 20–80 hydrogel mixture was prepared as described above in handmade cylindrical silicon molds of 10 mm diameter with a solution volume of 250 μL. After 30 min of crosslinking at 37 °C, the samples were soaked in dPBS for 24 h until equilibrium. They were then cleaned 3 times with milliQ water, frozen with liquid nitrogen for 2 min and lyophilized to obtain the scaffolds. The upper layer of the samples was peeled off with a scalpel to expose the pores. The scaffolds were stored in a dry environment until use.

2.4. Hydrogels and scaffold characterization: rheology, swelling and morphology

A Discovery HR-2 hybrid rheometer (TA Instruments) was used to perform the rheological experiments at 37 °C. The solvent trap geometry avoided water loss during the measurements. Parallel plates of 20 mm diameter with an intervening gap of 1100 μm were used for the hydrogels. Gelation kinetics was recorded *in situ* by the addition of H_2O_2 to the mixture of polymer and HRP, previously placed in the lower plate of the device. The experiments had three steps: a time sweep for 45 min (strain and frequency fixed at 1 % and 1 Hz, respectively) to determine gelation time, an amplitude sweep from 0.01 % to 20 % (frequency at 1 Hz) to fix the linear viscoelastic region and a frequency sweep to characterize crosslinked hydrogels from 0.1 Hz to 10 Hz (strain at 1 %). Rheology of Gel-HA scaffold equilibrated in culture media was performed with parallel plates of 12 mm diameter. The gap between plates was adjusted manually for each replicate, fixing an axial force of approximately 0.1 N. The protocol consisted of the same amplitude and frequency sweeps as for the hydrogels.

The equilibrium water content of the hydrogels was characterized by cylindrical samples prepared in molds of 10 mm diameter with precursor solutions of 250 μL. Once crosslinked, the hydrogels were immersed in dPBS 1× at 37 °C for 24 h until equilibrium. After rinsing the hydrogels three times with milliQ water they were weighed to obtain the swollen mass (m_w) and lyophilized to obtain the dry mass (m_d). Equilibrium water content (w) was calculated in reference to the dry mass by Eq. (1):

$$w = \frac{m_w - m_d}{m_d} \quad (1)$$

The volumetric swelling ratio (Q_v) was calculated with the data of w as in [35].

The swelling capacity of the scaffold was also determined by swelling different replicates of dry scaffolds in the same conditions as the hydrogels.

Scaffold morphology was characterized by observing cross-sections with a field emission scanning electron microscope (FESEM) (Ultra 55, Zeiss) at an acceleration voltage of 2 kV. Sample sections were obtained with a blade and were sputter coated with platinum previously to the observation. Images were treated with ImageJ software (FIJI) to obtain the mean pore size and area of the scaffold.

2.5. Culture of HepG2 cells in Gel-HA hydrogels

HepG2 cell line was cultured in Ham's F-12/Leibovitz L-15 medium (1:1 *v*/v) (supplemented with 7 % newborn calf serum (NCS), penicillin (50 U /mL) and streptomycin (50 μg /mL). HepG2 cells were detached using 0.25 % trypsin/0.02 % EDTA at 37 °C.

Solutions of different ratios (100–0, 80–20, 50–50, 20–80 and 0–100 vol/vol) of Gel+HRP and HA + HRP were prepared as previously described. Cells (200,000 cells/hydrogel) were added to each Gel-HA mixture. Finally, 90 μL of the Gel-HA cell suspension were crosslinked with 10 μL of H_2O_2 (20 mM) on each culture plate well, resulting hydrogels of 100 μL. Viability was determined by incubating the cultures with Hoechst 33342 (1.5 μg/mL) and PI (1.5 μg/mL) for 30 min. The culture medium was then removed and the samples observed under a fluorescence microscope using the appropriate filters (INCELL6000 Analyzer). Non-viable cells were recognized by their positive red fluorescence (PI) in the nuclei. The acquired images were analyzed by the INCELL Workstation module. Background correction was applied to all the images before being quantified. Cell count was determined from the Hoechst 33342 staining. An edge detection algorithm was used to define the nucleus as the main object. To separate individual cells, segmentation was applied.

HepG2 cells in monolayers (2D) were always used in parallel to determine if the 3D culture influence the performance of the cells. For this purpose, HepG2 cells were seeded in 24-wells plates at a density of 1.6×10^5 cells/cm^2.

2.6. Hepatocyte isolation and culture

Liver tissue samples were obtained in accordance with the principles of the Declaration of Helsinki and after the approval of the hospital's Ethics Committee (2019/00111/PI). Informed consent was obtained from all subjects involved in the study. PHH were isolated from cadaveric livers using a two-step collagenase perfusion procedure. Cellular viability was assessed by the dye exclusion test with 0.4 % trypan blue. PHH were cryopreserved in ice-cold Cell Banker medium as previously described [36] at a density of 10^7 viable cells/mL. The cells were thawed (after being stored in liquid nitrogen for at least 2 weeks) in the standard medium and were centrifuged at 100 *g* for 3 min. Hepatocytes were seeded and cultured as previously described in detail [37,38]. The PHH culture medium consisted of Ham's F-12/Williams medium (1:1) supplemented with NCS (2 %), BSA (1 g/L), L-glutamine (2.5 mM), glucose (17 mM), transferrin (25 μg/mL), ascorbic acid (0.62 mM), ethanolamine (66.8 μM) linoleic acid (7.7 μM), N-omega-nitro-L-arginine methyl ester (0.64 mM), insulin (10^{-8} M), penicillin (50 U/mL) and streptomycin (50 μg/mL) as previously described [39].

Following ethanol sterilization, the scaffolds were washed in sterile deionized water and maintained in F12 medium for 24 h. The culture medium was removed and two million viable cryopreserved/thawed human hepatocytes were added to the scaffold. The culture medium was added after 1 h and viability and hepatic functionality were evaluated after 24 h of culture.

The PHH monolayers were always used in parallel to determine whether the 3D culture influenced the cell performance, for which the PHH were seeded in 24-well plates at a density of 1.3×10^5 viable cells/cm^2.

2.7. Assessment of hepatic functionality and drug-metabolism

The formation of urea from NH_4^+ (ureogenic capacity) was determined in 2D or 3D cultures as previously described in detail [37]. Eight different cytochrome P450 (CYP) activities (CYP1A2, CYP2A6, CYP2B6, CYP2C9, CYP2C19, CYP2D6, CYP2E1 and CYP3A4) were simultaneously assayed by incubation with a cocktail of selective substrates for individual P450 isoenzymes, as previously described [40,41]. UDP-glucuronosyltransferase (UGT) activities were assayed by incubating cultured cryopreserved/thawed hepatocytes with the corresponding selective substrates: 15 μM β-estradiol or 250 μM naloxone for determining UGT1A1 or UGT2B7, respectively [42]. The corresponding metabolites formed after incubation were evaluated by high-performance liquid chromatography/mass spectrometry (HPLC/MS), as previously described in detail [40–42].

The human albumin sandwich enzyme-linked-immunosorbent assay (ELISA) quantification kit (Bethyl Laboratories, USA) was used for measuring albumin production and secretion in the culture media, as described by the manufacturer.

2.8. Immunofluorescence

After 24 h in culture, samples were fixed with 4 % formaldehyde for 20 min and washed 3 times with DPBS. The scaffolds were sectioned to obtain better quality images. After fixing, the samples were immersed in 30 % sucrose-DPBS (wt/vol) overnight and then covered with OCT. Cryosections (40 μm) were obtained using the Leica CM 1860 UV cryostat, and then permeabilized using 0.1 % Triton ×100 in PBS for 20 min at room temperature, washed with PBS and blocked with DPBS containing 3 % BSA for 1 h at room temperature. The sections were then incubated overnight at 4 °C with an albumin primary antibody (Cell Signaling Technology, USA) diluted (1:100) in 1 % BSA-DPBS. The samples were washed three times and incubated for 1 h with a secondary antibody (anti-goat Alexa 488) (Invitrogen) (1:200) in 1 % BSA-DPBS, the sections were washed again three times and finally incubated with Hoechst 33342 (2 μg/mL) to detect nuclei. The sections were mounted in Gelmount solution imaged under a confocal microscope (Leica, DMI8). Specificity controls, performed by omitting the primary antibody, resulted in the abolition of immunostaining.

2.9. Acute liver failure (ALF) induction

Mice had free access to water and food and were housed in a temperature-controlled room with a 12-h dark/light cycle at the animal facilities of *Instituto de Investigación Sanitaria La Fe*. All the experimental procedures were approved by the Institutional Animal Ethics Committee (*Comité Ético de Bienestar Animal, Reference 2017/VSC/PEA/00069*), and followed the Spanish national and institutional regulations and EU Directive 2010/63/EU for animal experiments. All the animal experiments followed the ARRIVE guidelines. ALF was induced in male NOD/SCID mice (4–6 weeks) with a single dose of paracetamol (300 mg /kg) 16 h prior to cell transplantation and was initially evaluated by determining transaminases levels in sera and histological staining.

2.10. Intraperitoneal transplant of Gel-HA scaffolds containing hepatocytes in mice with ALF

The scaffolds were transplanted into the peritoneum of ALF animals 16 h after APAP injection. The animals were divided into four experimental groups: Groups 1 (control: non-treated animals), 2 (sham group:

animals with ALF and transplanted with cell-free scaffolds), 3 (transplanted with 2×10^6 PHH intrasplenically) and 4 (transplanted with Gel-HA scaffolds containing 2×10^6 PHH). For studying the therapeutic potential of the PHH-ladden scaffolds we used 2×10^6 (instead of 200,000 cells/hydrogel) because in the literature there is a wide diversity of cells used in LCT (ranging from 0.5×10^6 to 50×10^6 cells), but there is a minimum for detecting a significant recovery [43]. A sevorane/O_2 combination was used as anesthesia. All the mice were carefully monitored until recovery. At 1, 3 and 7 days after transplantation, the animals were sacrificed and blood and liver were collected for additional assessment. The blood samples were used to obtain serum after centrifuging and stored at −20 °C to determine human albumin levels by ELISA, transaminase levels and cytokine production. The liver samples were maintained in 4 % paraformaldehyde for pathological and immunofluorescence analyses or cryopreserved (−80 °C) for oxidative stress analyses.

2.11. Transaminases levels and histology

Alanine aminotransferase (ALT) and aspartate aminotransferase (AST) activities in sera were measured as an indication of liver function using a colorimetric kit (Sigma-Aldrich). AST and ALT activities were expressed as nmol/min/mL (milliunit/mL). Liver samples were embedded in paraffin and sectioned into 7 μm thick slices. The tissue samples were dyed with hematoxylin and eosin (H&E) after deparaffinization.

2.12. Determination of ophthalmic acid levels by mass spectrometry

Ophthalmic acid (OA) levels were determined in the liver tissue and sera by ultra-performance liquid chromatography coupled to mass spectrometry (UPLC-MS/MS) analysis, as previously described [44].

Briefly, frozen liver tissues (50–100 mg) were homogenized in six volumes (m/v) of PBS including N-ethylmaleimide (NEM 50 mM) in a Precellys 24 Dual system that contained a Cryolys cooler as previously described [44]. A second tissue extraction was performed consecutively using four volumes of PBS with 50 mM of NEM. Finally, both supernatants were joined and stored at −80 °C until analysis. For serum, 10 μL were thawed on wet ice before sample preparation. OA levels were analyzed using an UPLC-MS/MS. The data was processed on Waters MassLynx 4.1 software for quantitative analysis, as previously described [44].

2.13. Cytokine determination

Inflammation cytokines were analyzed in mouse serum samples (stored at −80 °C) by Luminex using a custom-designed multiplex cytokine magnetic bead panel (Merck-Millipore MHSTCMAG-70K), following the manufacturer's guidelines. Absolute cytokine concentrations were determined by a 5-parameter logistic curve fits. The sensitivity of each cytokine test was expressed in pg/mL.

2.14. Statistical analysis

The data represent triplicate measurements and are expressed as the mean ± SD. A Student's *t*-test was used for statistically evaluating pairs of groups and one-way ANOVA and post-Tukey's multiple comparison test to compare groups of three or more. The significance level was set at $p < 0.05$ and calculated on GraphPad Prism *vs.* 6.1.

3. Results

3.1. Gel-HA hydrogels

Gelatin and hyaluronic acid were grafted with tyramine to be enzymatically crosslinked with HRP and form hydrogels [35] (Fig. 1A). Tyramine grafting on the hydrogel precursor macromolecules was confirmed by UV spectrophotometry by the absorbance peak at 275 nm (Fig. S1). The tyramine degree of substitution [45] was similar in both polymers (1.68×10^{-7} mol Tyr/mg for Gel and 1.64×10^{-7} mol Tyr/mg for HA). Efficient grafting was supported by the FTIR spectra (see Fig. S2) in which the peak at 2950 cm^{-1} was more pronounced in the tyramine conjugates than in the pristine samples (aromatic C—H stretching [46,47]). Hydrogel mixtures were successfully synthesized in F12 medium (Fig. 1B). The gelatin was whitish (due to the formation of some physical crosslinks [48]), while the HA and mixtures were transparent. The mixture transparency indicated homogenous mixing of the two polymers [48].

The gelation times of the different hydrogels, determined from the evolution of the shear storage moduli (G') with the crosslinking time (see Fig. 1B) [35], are listed in Table 1. Gel crosslinked faster (6 min) than HA (20 min), with a significant statistical difference. The mixtures presented intermediate gelation times that increased with HA content. As the degree of tyramine grafting and the amount of HRP and H_2O_2 were the same for both Gel and HA, the differences in crosslinking times were probably due to the different viscosities of the polymeric solutions (Fig. S3).

The rheological properties of crosslinked hydrogels as a function of the frequency showed that the storage modulus G' (Fig. 1D) was much higher than the loss modulus G" (Fig. 1E), indicating hydrogel elasticity [33]. No significant variation of the values of G' with the frequency was found either in HA or the mixtures. A slight increase was seen in the Gel above 2 Hz, which could be an indication of a relaxation process [49]. A constant strain of 1 % within the linear viscoelastic region in which the complex modulus does not change with the strain was chosen for the measurements (Fig. S4).

Gel absorbed the lowest amount of water in equilibrium and HA the highest (32 g and 56 g of water per g of dry polymer, respectively) (Fig. 1F). The quantity of water in the mixtures increases with their HA content, as was found when crosslinking with *CF*-KRB [35]. The network expansion rose with HA content in the mixtures as did the volumetric swelling ratio (Table 1). Crosslinking density (ρ_x) (mol of chains per unit volume of polymer) was calculated as in [35], but considering that the hydrogels were crosslinked in an aqueous medium (relaxed state [50]) (Eq. (2)):

$$\rho_x = \frac{-ln(1-\phi_p) - \phi_p - \chi \cdot \phi_p^2}{v_w \phi_{p,r}^{2/3} \phi_p^{1/3}} \quad (2)$$

ϕ_p and $\phi_{p,r}$ being the volume fraction of polymer in the swollen and relaxed states, respectively, χ the Flory Huggins interaction parameter (0.49 for Gel [51] and 0.473 for HA [52]) and v_w the molar volume of water. Despite having different swelling capacities, all the samples had a similar crosslinking density (Table 1), consistent with the similar degree of Gel and HA tyramine grafting. HA's greater ability to absorb water than Gel is due to its higher hydrophilicity [35], expressed by the lower value of the Flory-Huggins parameter [51,52].

The G' values at a fixed frequency of 1 Hz (Fig. 1G-H) show that the Gel is very soft, G' = 36 Pa. However, as the content of HA in the mixtures increased, the modulus also rose significantly for samples 80–20 and 50–50, with values of 163 Pa and 245 Pa, respectively. A value of 375 Pa was obtained for the 20–80 sample. HA hydrogel presented the highest value (755 Pa) with significant difference among the remaining samples. The G' values were lower than when crosslinking in *CF*-KRB [33], probably due to the lower degree of oxidation of the phenol groups of tyramine. Since HA is the hydrogel that absorbs most water and all hydrogels have a similar crosslinking density, HA's greater stiffness than that of Gel could then be attributed to the higher rigidity of the HA chains [53] and the lower water permeability coefficient [54], as previously found when crosslinking in *CF*-KRB [35].

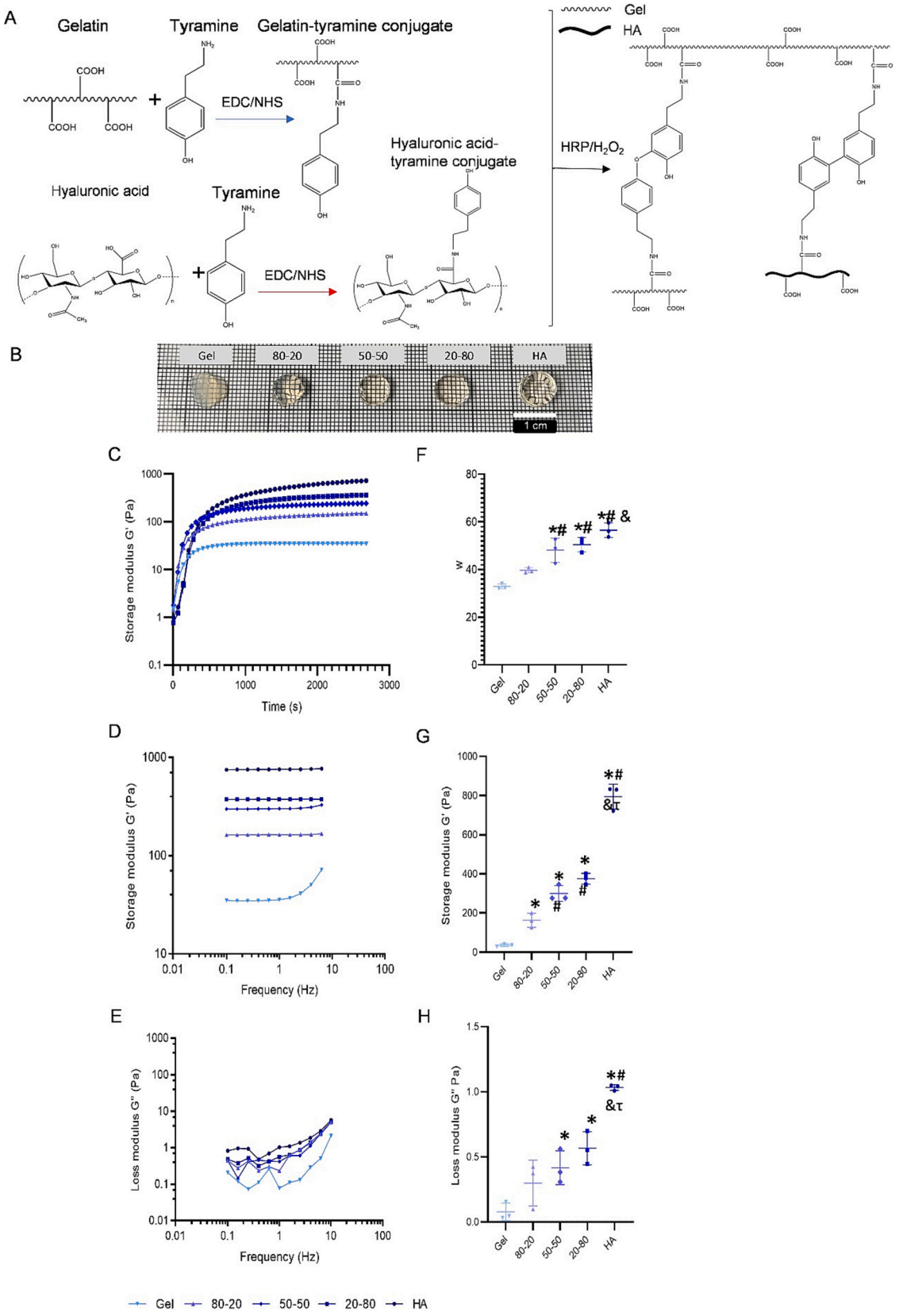

Fig. 1. Mechanical properties and swelling of Gel-HA hydrogels. (A) Chemical modification of gelatin and hyaluronic acid to graft tryamine molecules in the presence of EDC and NHS and subsequent hydrogel crosslinking mechanism by phenol oxidation with H_2O_2 catalyzed by the enzyme HRP. (B) Macroscopic image of Gel-HA hydrogels after crosslinking in molds. (C) Evolution of the shear storage modulus during the crosslinking in the rheometer at 1 Hz and 1 % strain ($n = 3$). (D) Storage (G') and (E) loss (G") modulus at 1 % strain as a function of the frequency of the crosslinked Gel-HA hydrogels. (F) Equilibrium water content (w) of Gel-HA hydrogels after 24 h in dPBS. (G) Storage (G') and (H) loss (G") modulus at 1 Hz and 1 % strain of the crosslinked Gel-HA hydrogels. *At least $p \leq 0.01$ (compared to

Gel); $^{\#}p \leq 0.001$ (compared to 80–20); $^{\&}p \leq 0.01$ (compared to 50–50); $^{\tau}p \leq 0.001$ (compared to 20–80); (n = 3; ANOVA followed by Tukey's multiple comparisons test).

Table 1
Main properties of Gel-HA hydrogels.

Gel-HA	Gelation time (min)	Swelling Ratio	Crosslinking density (mol/m^3)
100–0	6 ± 1	48 ± 1	22 ± 2
80–20	9 ± 1	56 ± 2	20 ± 1
50–50	13 ± 4*	64 ± 6*	21 ± 3
20–80	16 ± 3*,#	65 ± 3*	23 ± 3
0–100	20 ± 1*,#,&	70 ± 3*,#	22 ± 2

* At least p ≤ 0.01 (compared to Gel).
# p ≤ 0.001 (compared to 80–20).
& p ≤ 0.01 (compared to 50–50); (n = 3; ANOVA followed by Tukey's multiple comparisons test).

3.2. Optimization of the composition of Gel-HA hydrogels

To determine the optimal Gel-HA composition for hepatic cell culture, HepG2 cells were encapsulated in the different hydrogel compositions. Despite the long crosslinking times of the HA-rich compositions, the high viscosity of the solutions prevented the cell suspension sinking below the hydrogel, with a homogeneous distribution of cells within the entire hydrogel volume (Fig. S6). The F12 medium allowed proper crosslinking compatible with HepG2 cell culture. No significant differences were found in viability (Fig. 2A-B), although increased ureogenic capability, a specific hepatic function, was detected in the HA-rich hydrogels (Fig. 2C), indicating an advantage for hepatic cell culture. Comparable results were observed in albumin synthesis and secretion into the culture media of HepG2 cells encapsulated in hydrogels with different Gel-HA compositions (Fig. 2D). These results are in agreement with other researchers that have shown increased functionality of hepatic cells cultured in HA [55,56]. These results, together with the analyzed mechanical properties, led us to select the 20–80 Gel-HA composition as the optimal for hepatic cell culture due to its storage modulus G' of 375 Pa being very close to the range of the human liver (400 to 600 Pa [57,58]).

3.3. Gel-HA scaffolds increase the functionality of primary human hepatocytes in vitro

Scaffolds were obtained by lyophilizing Gel-HA 20–80 hydrogels. Fig. S5A shows the evolution of the shear storage modulus with frequency and compared with the hydrogel of the same composition (20–80). At 1 Hz G' of the scaffold (752 Pa) is higher than that of the hydrogel (375 Pa) though still close to the upper range of the modulus of human liver [57,58]. The scaffold's equilibrium water content was significantly lower than that of the hydrogel (Fig. S5B), probably due to the more efficient crosslinking in *CF*-KRB, which also explains the enhanced mechanical properties.

The scaffold morphology (Fig. 3A) consisted of an interconnected honeycomb-like porous structure typical of hydrogels made of natural origin polymers [59], with mean pore sizes of 102 ± 36 μm and mean pore area of 5211 ± 3910 μm^2. The high dispersion of the area results are due to the non-homogeneous pore shapes (see Fig. 3A).

For clinical applications, PHH should maintain key hepatic functions such as detoxification capacity or ureogenesis. PHH were cultured in Gel-HA 20–80 scaffolds and cell viability and functionality were assessed and compared to monolayer cultures after 24 h of culture, at which time they would be transplanted into the host after proper stabilization [12,60]. The viability of cryopreserved/thawed PHH used for 3D culture was higher than 80 %. 24 h after seeding PHH in Gel-HA scaffolds the viability was maintained (78 %). Immunofluorescence of scaffold sections revealed that PHH express key hepatic markers such as albumin and that they maintained cell-cell interactions homogeneously distributed throughout the scaffolds (Fig. 3B). It can be seen that the non-homogeneous shape of the scaffold pores that gave rise to an area of highly dispersed pores do not negatively influence cell distribution.

Ureogenesis, albumin secretion and phase I and II activities were evaluated to determine whether cultivating PHH in Gel-HA scaffolds maintained specific hepatic functions. The functional activities of CYP1A2, CYP2A6, CYP2B6, CYP2C9, CYP2C19, CYP2D6, CYP2E1 and

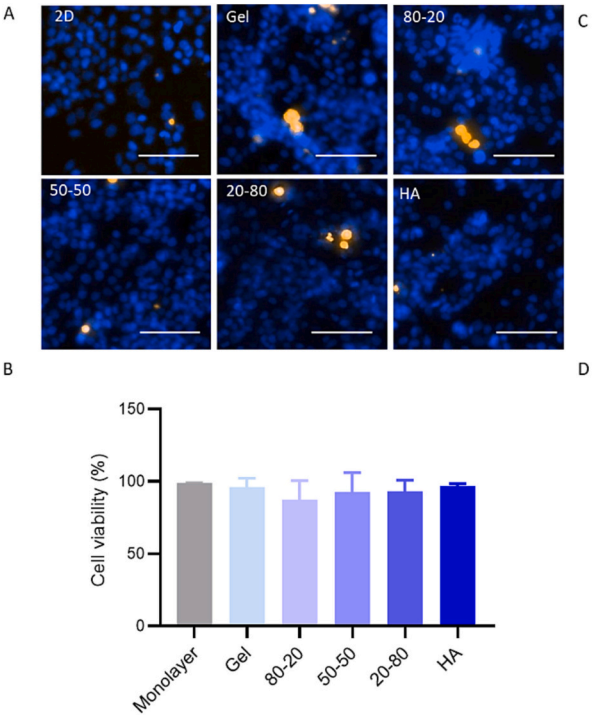

Fig. 2. *In vitro* assessment of Gel-HA hydrogels with HepG2 cells. (A) Representative images of live-dead assays of HepG2 cells in Gel-HA hydrogels after 24 h of culture. Scale bar = 100 μm. Nuclei were detected by Hoechst 33342 (blue) staining in all the images. Dead cells were identified by propidium iodide staining (orange). (B) Quantification of cell viability after 24 h of culture. (C) Ureogenic capability of HepG2 encapsulated in Gel-HA. (D) Albumin synthesis in different culture conditions. *At least $p \leq 0.01$ (compared to monolayer); $^{\#}p \leq 0.001$ (compared to Gel); $^{\&}p \leq 0.01$ (compared to 80–20); $^{\tau}p \leq 0.001$ (compared to 50–50); $^{\Psi}p \leq 0.001$ (compared to 20–80); ($n = 6$; ANOVA followed by Tukey's multiple comparisons test).

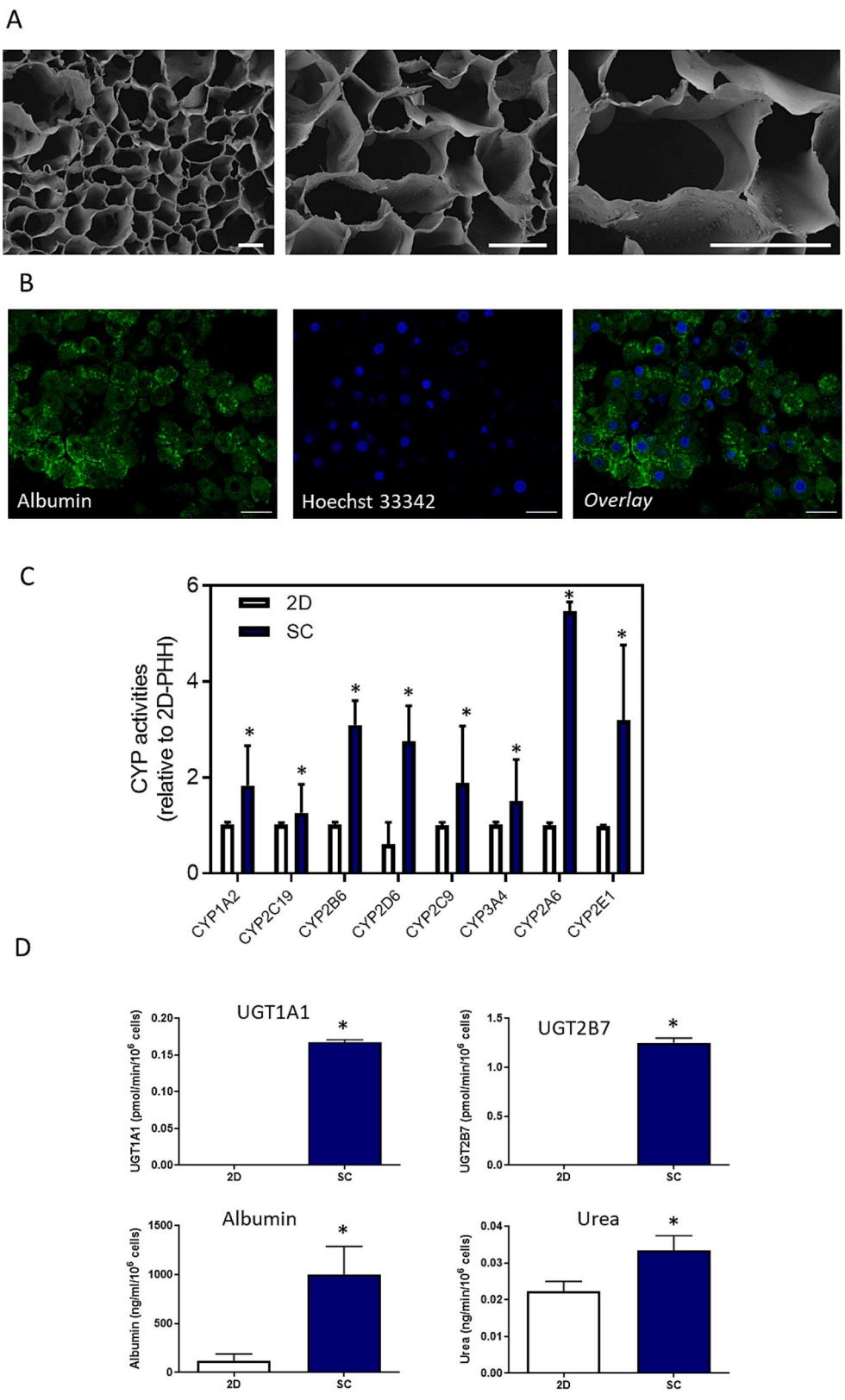

Fig. 3. *In vitro* culture of PHH in Gel-HA scaffolds. (A) FESEM representative images of Gel-HA scaffolds. (B) Immunofluorescence of human albumin in scaffold sections. Nuclei were identified by staining with Hoechst 33342. (C) CYP activities levels in PHH cultured in Gel-HA scaffolds (SC) and compared to PHH cultured on monolayers (2D). (D) Comparative functionality (UGT1A1 and UGT2B7 activity levels, synthesis and secretion of albumin, ureogenic capacity) of PHH cultured in 2D or SC after 1 day in culture. *At least $p \leq 0.05$ (Student's *t*-test compared to 2D cultures). Scale bar (100 μm) applies to all the images.

CYP3A4 were higher in PHH-scaffolds than 2D cultures (Fig. 3C). Higher activity levels of the PHH cultured in scaffolds were detected for CYP2A6, CYP2B6 and CYP2D6. When phase II drug metabolizing enzymes (UGT1A1, UGT2B7) activities were analyzed we only detected enzymatic activities in hepatocytes cultured in scaffolds, which confirms the advantage of using a 3D culture over instead of monolayers for culturing PHH (Fig. 3D).

The PHH-scaffolds also showed a significantly higher ureogenic capability than the monolayer cultures. Human albumin secreted into the media showed a significant increase in PHH cultured within scaffolds than in those cultured in 2D (Fig. 3D).

3.4. Transplantation of Gel-HA scaffolds seeded with PHH rescues mice with acetaminophen-induced liver failure

An ALF animal model was used to assess the effects of PHH-laden scaffolds *in vivo*. A single dose of acetaminophen (APAP) at 300 mg/kg was lethal in 56 % of the treated mice 1 week after damage induction, whereas all the transplanted animals (with cells administered intrasplenically or scaffolds containing cells) survived, indicating a survival benefit for the animals that had a liver cell transplant (Fig. 4A). The histopathological analysis of liver tissue of the different animal groups revealed significant differences among them: those in the APAP group showed massive hepatic centrilobular necrosis, necroinflammation and degeneration, while the livers of those in the APAP+C and APAP+SC groups had a reduction of the necrotic areas and no signs of necroinflammation (Fig. 4B).

Increased AST and ALT levels indicated hepatocyte damage after APAP injection. The transplanted animals had a reduction in transaminases levels. It should be noted that this reduction was significantly higher in animals treated with scaffolds containing PHH (APAP+SC) than in those that received PHH (APAP+C) only intrasplenically after 1 and 3 days (Fig. 4C).

Human albumin was detected in the sera of the transplanted mice, indicating the transplantion success (Fig. 4D). The human albumin levels were higher in animals transplanted with PHH-scaffolds (APAP+SC) than in those that received cells only (APAP+C). These albumin levels were maintained for up to 30 days after transplant (data not shown). As expected, non-measurable human albumin was found in non-transplanted animals (control and sham group).

3.5. Transplantation of Gel-HA scaffolds with PHH results in a reduction of liver oxidative stress and reduced inflammatory response induced by acetaminophen

GSH depletion and oxidative stress induction have been defined as key mechanisms involved in APAP-induced toxicity. Moreover, increased glutathione analogue ophthalmic acid (OA) has been described after APAP administration [61]. The differential metabolomics study revealed significantly higher OA levels in the livers of APAP-treated mice than in the control animals, while significantly reduced levels were identified in transplanted animals (Fig. 5A), with the animals transplanted with PHH-scaffolds (APAP+SC) showing the lowest OA levels. To look for a possible non-invasive biomarker of the success of liver cell transplantation, the levels of OA were analyzed in the sera of the different experimental groups. Increased OA levels were found in the serum of animals with APAP-ALF, while they were reduced in the animals that had ALF and a PHH transplant (Fig. 5B). Interestingly, the reduction was significantly higher in the animals transplanted with scaffolds (APAP+SC) than in those that were intrasplenically transplanted with PHH (APAP+C), which agrees with the reduction of key hepatic markers such as transaminases levels. These results indicate that OA levels could be a potential indicator of the therapeutic effectiveness of cell therapy.

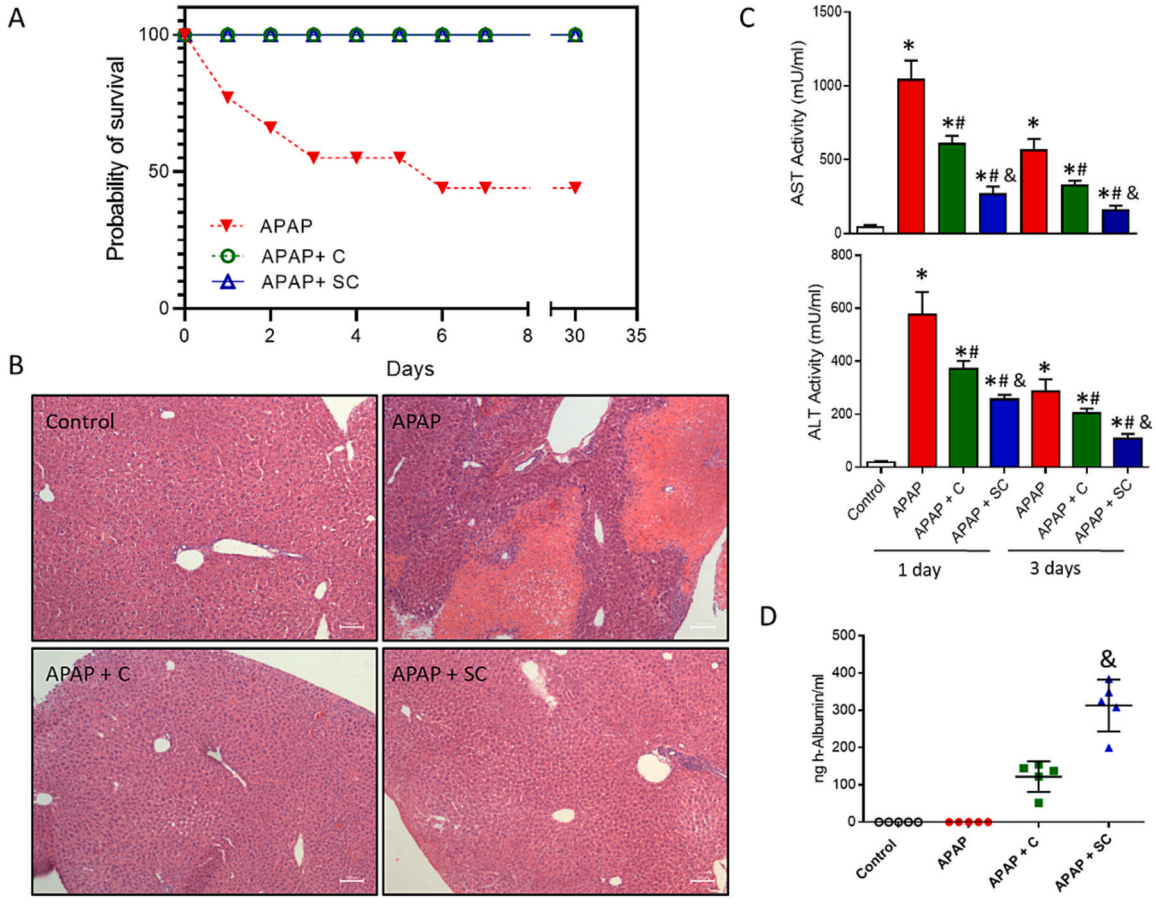

Fig. 4. *In vivo* effects of primary human hepatocytes after intrasplenic transplantation or intraperitoneal administration of Gel-HA scaffolds in SCID mice with acute liver failure (ALF). (A) Survival of transplanted animals compared to sham mice. (B) Histological analysis of liver tissue in treated animals. (C) Transaminases levels (ALT and AST) in mice after ALF or mice transplanted with cells (C) or scaffolds (SC) containing PHH 1 or 3 days after transplantation. *At least $p \leq 0.05$ (compared to control animals); $^{\#}p \leq 0.01$ (compared to APAP treated animals); $^{\&}p \leq 0.01$ (compared to APAP treated animals transplanted with PHH intrasplenically (APAP+C)) (ANOVA followed by Tukey's multiple comparisons test). (D) Human albumin levels in the serum of transplanted animals. $^{\&}$At least $p \leq 0.001$ (compared to APAP-treated animals transplanted with PHH intrasplenically; Student's t-test).

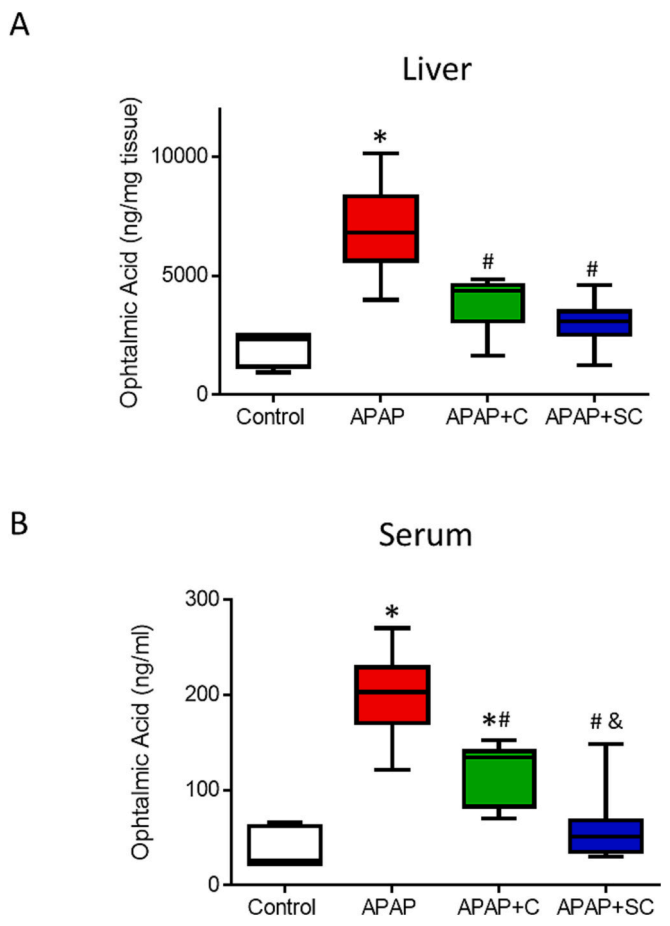

Fig. 5. Transplantation of scaffolds containing PHH reduces ophthalmic acid levels after ALF. (A) Ophthalmic acid (OA) levels in the liver of APAP mice receiving PHH intrasplenically (APAP+C) or transplanted intraperitoneally scaffolds with PHH (APAP+SC) 24 h after treatment. (B) OA levels in the serum of the different experimental groups. *At least $p \leq 0.05$ (compared to control animals); $^{\#}p \leq 0.01$ (compared to APAP treated animals); $^{\&}p \leq 0.01$ (compared to APAP treated animals transplanted with PHH intrasplenically (APAP+C)) (ANOVA followed by Tukey's multiple comparisons test).

Augmented levels of pro-inflammatory cytokines have been described after an APAP overdose [62]. The levels of CXCL1, IL-6, TNF-α and IFN-γ were analyzed in the serum of the transplanted animals. Increased cytokine levels were noted in animals after APAP administration, while there was a reduction of these levels after PHH transplantation (Fig. 6). The levels of CXCL1 were significantly lower in animals transplanted with PHH-scaffolds (APAP+SC) than in those transplanted with PHH (APAP+C). This reduction in the PHH-scaffold animals was also identified for IL-6 and TNF-α compared to the APAP animals, although this reduction was not significantly different to that in the PHH-mice. Finally, increased IFN-γ levels were found in APAP-treated animals but there were no significant changes in the transplanted animals.

4. Discussion

Liver transplant is currently the only effective treatment for end-stage liver diseases, although it is limited by the scarcity of liver tissue, which has led to a search for alternative therapeutic approaches such as cell transplants. Engraftment inefficiency poses an important challenge for the clinical outcome of liver cell therapy and limits its more extensive use. The main objective of this study was to study the advantages of transplanting banked human hepatocytes seeded in Gel-HA scaffolds over intrasplenically transplanted PHH in APAP-overdosed mice, an animal model of ALF, to correct hepatic disease. We found a significantly more efficient ALF correction when PHH are transplanted in Gel-HA scaffolds, providing essential mechanistic information.

Rheological measurements of bulk human liver show that the storage modulus of the tissue ranges from 400 to 600 Pa [57,58], the range of matrix rigidities in which hepatocytes should exhibit optimal liver-specific functionalities. Previous studies in HA hydrogels containing liver ECM found higher levels of hepatocyte gene expression and higher levels of albumin secretion in hydrogels with shear moduli of 600 Pa and 1200 Pa, which declined significantly in stiffer substrates of 4600 Pa [55]. In our case, the Gel-HA 20–80 mixture had a G' value of 375 Pa, which is close to 400 Pa and was chosen as the optimal for hepatic cell culture and scaffold preparation. The advantage over pure HA, whose modulus is also close to the range of the natural tissue, is that combined compositions contain Gel molecules that are bioactive and provide cell adhesion [63].

Porosity and pore size have a considerable effect on cell regeneration and functionality. Previous reports have suggested a pore size of 50–200 μm for the culture of hepatocytes [64–66]. For freeze-dried scaffolds, optimal pore size for hepatocyte culture was higher than 100 μm [67]. The same order of magnitude, 82 μm, was also optimal for rat hepatocytes cultured on collagen scaffolds [66]. Our results show that the scaffold is composed of interconnected honeycomb shaped pores of 102 μm mean size, which seems suitable for hepatocyte culture. Since our scaffold's mechanical shear modulus is close to the upper range of the native liver (752 Pa), the proper cell stimulation can be expected.

Our results agree with those that have previously showed that hepatocytes cultured in 3D constructs have better functionality than cells cultured on monolayer [11,15]. HepG2 cells were used to select the most suitable composition. Encapsulation of hepatic cells in Gel-HA hydrogels enhanced their functionality and optimal viability for all the compositions, although HA-richer compositions with mechanical properties within the range of human liver seemed to increase the ureogenic capacity. By modulating the composition of the hydrogels, the nature of the interaction of cells with the hydrogel is also modified, which can also influence cell functionality. HepG2 cells interaction with collagen, from which Gel derives, is mediated by the $\alpha_2\beta_1$ integrin [68], while in HA the interaction occurs through the cell-surface glycoprotein receptor CD44 [69,70].

Hepatocytes are the major cell type in the adult liver and play crucial functions, including plasma protein secretion, ureogenesis or detoxification [71]. Most studies use the measurement of urea and albumin as markers of functionally efficient transplanted cells, although there is no standardization of the acceptable concentrations for function [30], while complete, and exhaustive characterization of cellular products is mandatory before their clinical application. In this paper, the results indicate that although no significant differences in viability between 2D and 3D cultures were found, a complete characterization of the cellular systems revealed important additional improvements in culturing hepatic cells in Gel-HA hydrogels or scaffolds. Urea formation is an essential and specific hepatic function for the removal of the ammonia generated from protein catabolism and it has also been found to be a suitable indicator of mitochondria preservation [38]. On the other hand, detoxification, one of the liver's major functions, involves both waste removal and xenobiotic biotransformation and is of special interest for the clinical application of hepatocyte transplantation for patients receiving broad medication. The improved ureogenic capacity, albumin production and metabolic performance of the cells (Fig. 3) is thus very likely to confer an advantage to scaffolds *in vivo*. Although a difference was found in the mechanical properties of the hydrogel and the scaffold, it did not have a negative impact on cell behavior, as both HepG2 and PHH had better hepatic functionality than the monolayer cultures.

An acetaminophen overdose is a common cause of acute liver injury and supplies a model compound for preclinical studies, since the molecular mechanisms involved in APAP-induced toxicity have been

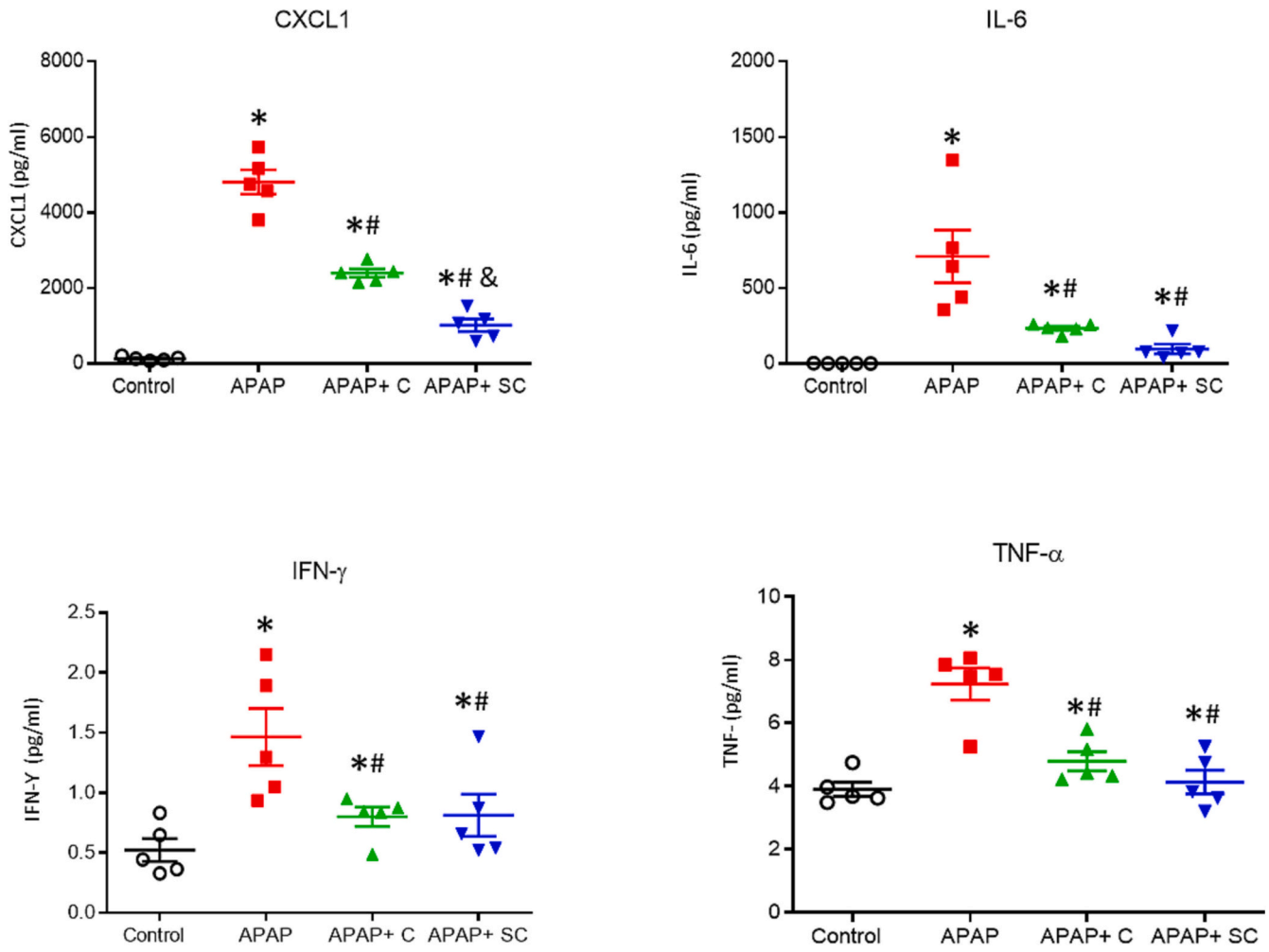

Fig. 6. Transplantation of PHH-scaffolds reduces proinflammatory cytokines after ALF. Serum concentrations of proinflammatory cytokines (CXCL1, IL-6, IFN-γ and TNF-α) were determined by Luminex in the different animal groups 24 h after transplantation. *At least $p \leq 0.05$ (compared to control animals); $^{\#}$ $p \leq 0.01$ (compared to APAP treated animals); $^{\&}$ $p \leq 0.01$ (compared to APAP treated animals transplanted with PHH intrasplenically (APAP+C)) (ANOVA followed by Tukey's multiple comparisons test).

described in detail [72]. *N*-acetylcysteine is an effective treatment although if administered >10 h after ingestion and patients may develop ALF. Although organ transplant is the only effective ALF treatment, liver cell therapy could offer enough time to regenerate the patient's liver by recovering some essential liver functions. In our system, administering APAP produced ALF, characterized by a reduced survival and higher levels of ALT, AST and proinflammatory cytokines. While administering PHH reduced transaminases levels, PHH-laden scaffolds gave better results, probably the cells better conserving functionality, which was retained in the host liver. These results agree with those found in rats with ALF induced by galactosamine, in which transplanting hepatocytes encapsulated in alginate microbeads reduced the severity of the damage [19], although our system has the advantage of using biodegradable materials present in the liver ECM. Gel enables cell adhesion and HA provides stiffness and hydration. Le Guilcher et al. recently described pullulan-dextran hydrogels seeded with the HepaRG cell line for treating mice with APAP-induced ALF and found a that transplanted animals had a survival advantage over non-transplanted [73]. However, treatment with a cell line from a tumorigenic background would be difficult to transfer to a clinical setting. Also, although pullulan and dextran are biocompatible and biodegradable, liver ECM components such as collagen or HA would also help to improve different hepatic functions. On the other hand, ALF induction by APAP increased the levels of proinflammatory cytokines, as has been described for other types of ALF such as that induced by CCl4 administration [74], so that monitoring cytokine levels could also be an optimal approach for assessing cell transplantation's effectiveness, since they were significantly reduced after transplanting PHH-laden scaffolds.

Acute liver failure is defined as hepatocellular necrosis and inflammation leading to liver failure. In the animal model studied, we showed that an APAP overdose that produced necrosis in the liver tissue could be reduced by cell therapy. APAP hepatotoxicity is known to be initiated by the formation of the *N*-acetyl-p-benzoquinone imine reactive metabolite, which reduces cellular glutathione (GSH) and produces protein adducts that finally induce oxidative stress and mitochondrial injury [75]. OA is a GSH analog in which the SH group of the cysteine is replaced by 2-aminobutyrate. Significant differences in the levels of OA were found after APAP administration, which agrees with previous observations in both animal models and humans after an overdose of paracetamol [61,76]. Interestingly, there was a statistically significant reduction in these levels in tissue and serum after a PHH transplant, suggesting that OA could also be a valuable biomarker of liver cell transplant the effectiveness of in ALF, since OA levels have also been associated with the clinical outcome of ALF.

The advantages of the scaffold method over intrasplenic administration have also been attributed to the different PHH delivery effectiveness of the intrasplenic and scaffold transplant system, since a higher percentage of cells (>70 %) are rapidly removed by phagocytes and

macrophages in intrasplenic infusion, [29,77]. In classical cell transplants the cells need to be transplanted into the spleen or liver parenchyma of animals or in the portal venous systems in humans, which is a high-risk method. PHH-laden scaffolds offer a safe method for enhancing the retention and function of PHH, as confirmed by biochemical and histological analysis, indicating that Gel-HA scaffolds could significantly improve the therapeutic effect of PHH on ALF by enhancing delivery and retention and extending the long-lasting effects. Delivered Gel-HA scaffolds also reduced the APAP-induced inflammatory response and oxidative stress better than the traditional intrasplenic administration of PHH. A proof of concept using bigger scaffolds should be previously carried out before transferring the technology to humans. Instead of using large scaffolds that could compromise cell oxygenation, microsphere-embedded cells could be implanted in a similar way, as reported by Dhawan [18]. Microsphere manufacture could be scaled up by using microfluidic systems [78] or by emulsion crosslinking [79], both have been previously applied in enzymatic hydrogels.

The shortage of available organs to isolate cells with enough quality and the low PHH engraftment after transplanting into the host liver limits the wider application of hepatocyte transplants. Our scaffold-based strategy allows retention of the cells and improved hepatic functions, although PHH availability would still be a limitation [9,80]. Other cell sources such as pluripotent stem cells differentiated into hepatic phenotypes could also be used as autologous therapies that would avoid immune rejection or could also be used to form biobanks of instantly available hepatocyte-like cells for the emergency treatment of different types of liver disease [9,81]. In this case, the Gel-HA would also enhance the functionality and performance of the differentiated cells, as has been previously shown with other 3D culture systems [11]. Overall, our results open up the possibility of testing other cell types, such as differentiated stem cells cultured in Gel-HA scaffolds, as alternative cell sources.

It should also be remembered that infiltrating monocytes and other liver cell types such as Kupffer cells plays a crucial role in liver homeostasis and immunity and contribute to liver pathology [82]. In this regard, as alternatively activated macrophages have been shown to reduce liver injury and inflammation in APAP-treated mice [72], using other cell types in scaffolds for liver disease should also be considered. Since no cell type includes all the requirements for effective regeneration, different authors have opted to explore the co-culture of different cell types. For instance, endothelial cells have been shown to induce not only vascularization but to stimulate liver organogenesis and regeneration [83,84]. Novel multi-cell type strategies would help to expand the application of liver cell therapy.

5. Conclusions

This paper describes a feasible PHH transplant technology based on the use of Gel-HA scaffolds to improve hepatic functions in an ALF mouse model as compared to traditional delivery methods such as intrasplenic injection. Biodegradable materials such as Gel and HA in clinical practice would offer an advantage over other strategies such as alginate microbeads [18,19]. Gel-HA scaffolds were prepared successfully to improve the functionality of human hepatocytes and also increased the efficacy of liver cell therapy *in vivo*. Mechanistically, PHH-scaffolds attenuate hepatocyte necrosis by reducing oxidative stress and the production of cytokines in mouse liver failure, thus increasing the survival rate. Both the pro-inflammatory cytokines and OA serum levels could be used as non-invasive biomarkers of the effectiveness of liver cell transplants in ALF treatment. The developed strategy would not only be a powerful tool in tissue engineering and regenerative medicine but could also be used for other applications such as disease modeling and drug screening, since the culture in Gel-HA enhances the performance of the hepatic cells.

Abbreviations

3D	three-dimensional
ALF	acute liver failure
ALT	alanine aminotransferase
APAP	acetaminophen
AST	aspartate aminotransferase
CYP	cytochrome P450
ECM	extracellular matrix
ELISA	enzyme-linked-immunosorbent assay
Gel	gelatin
HA	hyaluronic acid
HPLC/MS	high-performance liquid chromatography/mass spectrometry
NEM	N-ethylmaleimide
OA	ophthalmic acid
PHH	primary human hepatocytes
PI	propidium iodide
UGT	UDP-glucuronosyltransferase

CRediT authorship contribution statement

Conceptualization, M.S.·S, G.G.F., L.T.; methodology, J.R.F., E.G.L., E.V.B.; formal analysis, M.S.·S., G.G.F., L.T.; writing—original draft preparation, G.G.F., L.T.; supervision, M.S.S, G.G.F., L.T.; writing-review and editing, J.L.G.R., M.T.D., M.S.S., G.G.F., L.T.; funding acquisition, M.T.D., M.S.S., G.G.F., L.T. All authors have read and agreed to the published version of the manuscript.

Funding

This work has been supported by the Institute of Health Carlos III (Plan Estatal de I+D+i 2013-2016) and co-financed by the European Regional Development Fund "A way to achieve Europe" (FEDER) through grants PI18/00993, PI21/00223 and CP16/00097; by the Spanish Ministry of Science and Innovation MCIN/AEI/10.13039/501100011033 through the PID2019-106000RB-C21 and PID2019-106000RB-C22 Grants and by the Generalitat Valenciana (PROMETEO/2019/060). L.T. was supported by ISCIII CP16/00097 and MV21/00044, E.V.B through grant FI22/00082 (ISCIII). M.S-S was supported by an EPSRC Programme Grant (EP/P001114/1).

Declaration of competing interest

The authors declare that they have no known competing financial interests or personal relationships that could have appeared to influence the work reported in this paper. The funders had no role in either the design of the study, the collection, analyses, or interpretation of data in writing the manuscript or in the decision to publish the results.

Data availability

The raw/processed data required to reproduce these findings cannot be shared at this time due to technical and time limitations. Data will be made available on reasonable request.

Acknowledgements

The authors are grateful for the technical support received from the Cytomics Unit, Analytical Unit and Animal Facilities from the *Instituto de Investigación Sanitaria La Fe, and the Microscopy Service of* the Universitat Politècnica de València.

Appendix A. Supplementary data

Supplementary data to this article can be found online at https://doi.

org/10.1016/j.bioadv.2023.213576.

References

[1] S.K. Asrani, H. Devarbhavi, J. Eaton, P.S. Kamath, Burden of liver diseases in the world, J. Hepatol. 70 (1) (2019) 151–171, https://doi.org/10.1016/j.jhep.2018.09.014.

[2] B.J. Dwyer, M.T. Macmillan, P.N. Brennan, S.J. Forbes, Cell therapy for advanced liver diseases: repair or rebuild, J. Hepatol. 74 (1) (2021) 185–199, https://doi.org/10.1016/j.jhep.2020.09.014.

[3] R. Adam, V. Karam, V. Cailliez, et al., 2018 annual report of the European Liver Transplant Registry (ELTR) - 50-year evolution of liver transplantation, Transpl. Int. 31 (12) (2018) 1293–1317, https://doi.org/10.1111/tri.13358.

[4] M.C. Hansel, R. Gramignoli, K.J. Skvorak, et al., The history and use of human hepatocytes for the treatment of liver diseases: the first 100 patients, Curr Protoc Toxicol 62 (2014) 14121–141223, https://doi.org/10.1002/0471140856.tx1412s62.

[5] V. Iansante, R.R. Mitry, C. Filippi, E. Fitzpatrick, A. Dhawan, Human hepatocyte transplantation for liver disease: current status and future perspectives, Pediatr. Res. 83 (1–2) (2018) 232–240, https://doi.org/10.1038/pr.2017.284.

[6] C.T. Nicolas, R.D. Hickey, H.S. Chen, et al., Concise review: liver regenerative medicine: from hepatocyte transplantation to bioartificial livers and bioengineered grafts, Stem Cells (2016), https://doi.org/10.1002/stem.2500.

[7] E. Pareja, M.J. Gomez-Lechon, L. Tolosa, Induced pluripotent stem cells for the treatment of liver diseases: challenges and perspectives from a clinical viewpoint, Ann. Transl. Med. (2020), https://doi.org/10.21037/atm.2020.02.164 (in press).

[8] V.Y. Soldatow, E.L. Lecluyse, L.G. Griffith, I. Rusyn, Models for liver toxicity testing, Toxicol Res (Camb) 2 (1) (2013) 23–39, https://doi.org/10.1039/C2TX20051A.

[9] L. Tolosa, E. Pareja, M.J. Gomez-Lechon, Clinical application of pluripotent stem cells: an alternative cell-based therapy for treating liver diseases? Transplantation 100 (12) (2016) 2548–2557, https://doi.org/10.1097/TP.0000000000001426.

[10] M.J. Gomez-Lechon, L. Tolosa, I. Conde, M.T. Donato, Competency of different cell models to predict human hepatotoxic drugs, Expert Opin. Drug Metab. Toxicol. 10 (11) (2014) 1553–1568, https://doi.org/10.1517/17425255.2014.967680.

[11] P. Godoy, N.J. Hewitt, U. Albrecht, et al., Recent advances in 2D and 3D in vitro systems using primary hepatocytes, alternative hepatocyte sources and non-parenchymal liver cells and their use in investigating mechanisms of hepatotoxicity, cell signaling and ADME, Arch. Toxicol. 87 (8) (2013) 1315–1530, https://doi.org/10.1007/s00204-013-1078-5.

[12] M.J. Gomez-Lechon, M.T. Donato, J.V. Castell, R. Jover, Human hepatocytes in primary culture: the choice to investigate drug metabolism in man, Curr. Drug Metab. 5 (5) (2004) 443–462.

[13] V.Y. Soldatow, E.L. Lecluyse, L.G. Griffith, I. Rusyn, In vitro models for liver toxicity testing, Toxicol Res (Camb) 2 (1) (2013) 23–39, https://doi.org/10.1039/C2TX20051A.

[14] I.J. Fox, J.R. Chowdhury, Hepatocyte transplantation, Am. J. Transplant. 4 (Suppl. 6) (2004) 7–13, doi:340 [pii].

[15] A. Baze, C. Parmentier, D.F.G. Hendriks, et al., Three-dimensional spheroid primary human hepatocytes in monoculture and Coculture with nonparenchymal cells, Tissue Eng Part C Methods 24 (9) (2018) 534–545, https://doi.org/10.1089/ten.TEC.2018.0134.

[16] S. Gupta, K.K. Bhargava, P.M. Novikoff, Mechanisms of cell engraftment during liver repopulation with hepatocyte transplantation, Semin. Liver Dis. 19 (1) (1999) 15–26, https://doi.org/10.1055/s-2007-1007094.

[17] M. Grompe, E. Laconi, D.A. Shafritz, Principles of therapeutic liver repopulation, Semin. Liver Dis. 19 (1) (1999) 7–14, https://doi.org/10.1055/s-2007-1007093.

[18] A. Dhawan, N. Chaijitraruch, E. Fitzpatrick, et al., Alginate microencapsulated human hepatocytes for the treatment of acute liver failure in children, J. Hepatol. 72 (5) (2020) 877–884, https://doi.org/10.1016/j.jhep.2019.12.002.

[19] S. Jitraruch, A. Dhawan, R.D. Hughes, et al., Alginate microencapsulated hepatocytes optimised for transplantation in acute liver failure, PLoS One 9 (12) (2014), e113609, https://doi.org/10.1371/journal.pone.0113609.

[20] K.Y. Lee, D.J. Mooney, Alginate: properties and biomedical applications, Prog. Polym. Sci. 37 (1) (2012) 106–126, https://doi.org/10.1016/j.progpolymsci.2011.06.003.

[21] P.J. McKiernan, R.H. Squires, Bridging transplantation with beads in paediatric acute liver failure, Nat Rev Gastroenterol Hepatol 17 (4) (2020) 197–198, https://doi.org/10.1038/s41575-020-0281-0.

[22] A. Baiocchini, C. Montaldo, A. Conigliaro, et al., Extracellular matrix molecular remodeling in human liver fibrosis evolution, PLoS One 11 (3) (2016), e0151736, https://doi.org/10.1371/journal.pone.0151736.

[23] R.C. Benyon, M.J. Arthur, Extracellular matrix degradation and the role of hepatic stellate cells, Semin. Liver Dis. 21 (3) (2001) 373–384, https://doi.org/10.1055/s-2001-17552.

[24] G.S. van Tienderen, B. Groot Koerkamp, J.N.M. IJzermans, L.J.W. van der Laan, M. M.A. Verstegen, Recreating tumour complexity in a dish: organoid models to study liver cancer cells and their extracellular environment, Cancers (Basel) 11 (11) (2019), https://doi.org/10.3390/cancers11111706.

[25] G. Mazza, K. Rombouts, A. Rennie Hall, et al., Decellularized human liver as a natural 3D-scaffold for liver bioengineering and transplantation, Sci. Rep. 5 (2015) 13079, https://doi.org/10.1038/srep13079.

[26] S.K. Vishwakarma, A. Bardia, C. Lakkireddy, et al., Intraperitoneal transplantation of bioengineered humanized liver grafts supports failing liver in acute condition, Mater. Sci. Eng. C Mater. Biol. Appl. 98 (2019) 861–873, https://doi.org/10.1016/j.msec.2019.01.045.

[27] A.M. Syanda, V.I. Kringstad, S.J.I. Blackford, et al., Sulfated alginate reduces pericapsular fibrotic overgrowth on encapsulated cGMP-compliant hPSC-hepatocytes in mice, Front Bioeng Biotechnol 9 (2021), 816542, https://doi.org/10.3389/fbioe.2021.816542.

[28] J. Willemse, G. van Tienderen, E. van Hengel, et al., Hydrogels derived from decellularized liver tissue support the growth and differentiation of cholangiocyte organoids, Biomaterials 284 (2022), 121473, https://doi.org/10.1016/j.biomaterials.2022.121473.

[29] Y. Nagamoto, K. Takayama, K. Ohashi, et al., Transplantation of a human iPSC-derived hepatocyte sheet increases survival in mice with acute liver failure, J. Hepatol. 64 (5) (2016) 1068–1075, https://doi.org/10.1016/j.jhep.2016.01.004.

[30] M. Ali, S.L. Payne, Biomaterial-based cell delivery strategies to promote liver regeneration, Biomater Res 25 (1) (2021) 5, https://doi.org/10.1186/s40824-021-00206-w.

[31] R.A. Turner, E. Wauthier, O. Lozoya, et al., Successful transplantation of human hepatic stem cells with restricted localization to liver using hyaluronan grafts, Hepatology 57 (2) (2013) 775–784, https://doi.org/10.1002/hep.26065.

[32] J. Kumari, A.A. Karande, A. Kumar, Combined effect of cryogel matrix and temperature-reversible soluble-insoluble polymer for the development of in vitro human liver tissue, ACS Appl. Mater. Interfaces 8 (1) (2016) 264–277, https://doi.org/10.1021/acsami.5b08607.

[33] V. Moulisova, S. Poveda-Reyes, E. Sanmartin-Masia, L. Quintanilla-Sierra, M. Salmeron-Sanchez, G. Gallego Ferrer, Hybrid protein-glycosaminoglycan hydrogels promote chondrogenic stem cell differentiation, ACS Omega 2 (11) (2017) 7609–7620, https://doi.org/10.1021/acsomega.7b01303.

[34] J.J. Vaca-Gonzalez, S. Clara-Trujillo, M. Guillot-Ferriols, et al., Effect of electrical stimulation on chondrogenic differentiation of mesenchymal stem cells cultured in hyaluronic acid - gelatin injectable hydrogels, Bioelectrochemistry 134 (2020), 107536, https://doi.org/10.1016/j.bioelechem.2020.107536.

[35] S. Poveda-Reyes, V. Moulisova, E. Sanmartin-Masia, L. Quintanilla-Sierra, M. Salmeron-Sanchez, G.G. Ferrer, Gelatin-hyaluronic acid hydrogels with tuned stiffness to counterbalance cellular forces and promote cell differentiation, Macromol. Biosci. 16 (9) (2016) 1311–1324, https://doi.org/10.1002/mabi.201500469.

[36] M.T. Donato, M. Bolonio, E. Cabezas, et al., Improved in vivo efficacy of clinical-grade cryopreserved human hepatocytes in mice with acute liver failure, Cytotherapy 22 (2) (2020) 114–121, https://doi.org/10.1016/j.jcyt.2019.12.005.

[37] A. Bonora-Centelles, M.T. Donato, A. Lahoz, et al., Functional characterization of hepatocytes for cell transplantation: customized cell preparation for each receptor, Cell Transplant. 19 (1) (2010) 21–28, https://doi.org/10.3727/096368909X474267.

[38] L. Tolosa, E. Pareja-Ibars, M.T. Donato, et al., Neonatal livers: a source for the isolation of good-performing hepatocytes for cell transplantation, Cell Transplant. 23 (10) (2014) 1229–1242, content-cog_09636897_ct1036tolosa [pii], https://doi.org/10.3727/096368913X669743.

[39] M.J. Gomez-Lechon, A. Lahoz, N. Jimenez, J. Vicente Castell, M.T. Donato, Cryopreservation of rat, dog and human hepatocytes: influence of preculture and cryoprotectants on recovery, cytochrome P450 activities and induction upon thawing, Xenobiotica 36 (6) (2006) 457–472, https://doi.org/10.1080/00498250600674352.

[40] M.T. Donato, M.J. Gomez-Lechon, J.V. Castell, A microassay for measuring cytochrome P450IA1 and P450IIB1 activities in intact human and rat hepatocytes cultured on 96-well plates, Anal. Biochem. 213 (1) (1993) 29–33, doi: S0003269783713813 [pii].

[41] A. Lahoz, M.T. Donato, L. Picazo, M.J. Gomez-Lechon, J.V. Castell, Determination of major human cytochrome P450s activities in 96-well plates using liquid chromatography tandem mass spectrometry, Toxicol In Vitro 21 (7) (2007) 1247–1252. S0887-2333(07)00132-4 [pii], https://doi.org/10.1016/j.tiv.2007.03.022.

[42] M.T. Donato, S. Montero, J.V. Castell, M.J. Gomez-Lechon, A. Lahoz, Validated assay for studying activity profiles of human liver UGTs after drug exposure: inhibition and induction studies, Anal. Bioanal. Chem. 396 (6) (2010) 2251–2263, https://doi.org/10.1007/s00216-009-3441-1.

[43] H. Zhou, H. Liu, M. Ezzelarab, et al., Experimental hepatocyte xenotransplantation–a comprehensive review of the literature, Xenotransplantation 22 (4) (2015) 239–248, https://doi.org/10.1111/xen.12170.

[44] A. Carretero, Z. Leon, J.C. Garcia-Canaveras, et al., In vitro/in vivo screening of oxidative homeostasis and damage to DNA, protein, and lipids using UPLC/MS-MS, Anal. Bioanal. Chem. 406 (22) (2014) 5465–5476, https://doi.org/10.1007/s00216-014-7983-5.

[45] E. Sanmartín-Masiá, S. Poveda-Reyes, G. Gallego Ferrer, Extracellular matrix–inspired gelatin/hyaluronic acid injectable hydrogels, Int. J. Polym. Mater. Polym. Biomater. 66 (6) (2017) 280–288, https://doi.org/10.1080/00914037.2016.1201828.

[46] R. Egbu, S. Brocchini, P.T. Khaw, S. Awwad, Antibody loaded collapsible hyaluronic acid hydrogels for intraocular delivery, Eur. J. Pharm. Biopharm. 124 (2018) 95–103, https://doi.org/10.1016/j.ejpb.2017.12.019.

[47] N. Firouzi, A. Baradar Khoshfetrat, D. Kazemi, Enzymatically gellable gelatin improves nano-hydroxyapatite-alginate microcapsule characteristics for modular bone tissue formation, J. Biomed. Mater. Res. A 108 (2) (2020) 340–350, https://doi.org/10.1002/jbm.a.36820.

[48] S. Kripotou, K. Zafeiris, M. Culebras-Martinez, G. Gallego Ferrer, A. Kyritsis, Dynamics of hydration water in gelatin and hyaluronic acid hydrogels, Eur Phys J E Soft Matter 42 (8) (2019) 109, https://doi.org/10.1140/epje/i2019-11871-2.
[49] R. Kadri, G. Ben Messaoud, A. Tamayol, et al., Preparation and characterization of nanofunctionalized alginate/methacrylated gelatin hybrid hydrogels, RSC Adv. 6 (33) (2016) 27879–27884, https://doi.org/10.1039/C6RA03699F.
[50] N.R. Richbourg, N.A. Peppas, The swollen polymer network hypothesis: quantitative models of hydrogel swelling, stiffness, and solute transport, Prog. Polym. Sci. 105 (2020), 101243, https://doi.org/10.1016/j.progpolymsci.2020.101243.
[51] J. Baier Leach, K.A. Bivens, C.W. Patrick Jr., C.E. Schmidt, Photocrosslinked hyaluronic acid hydrogels: natural, biodegradable tissue engineering scaffolds, Biotechnol. Bioeng. 82 (5) (2003) 578–589, https://doi.org/10.1002/bit.10605.
[52] H.B. Bohidar, Hydrodynamic properties of gelatin in dilute solutions, Int. J. Biol. Macromol. 23 (1) (1998) 1–6, https://doi.org/10.1016/s0141-8130(98)00003-8.
[53] B.J. Kvam, M. Atzori, R. Toffanin, S. Paoletti, F. Biviano, 1H- and 13C-NMR studies of solutions of hyaluronic acid esters and salts in methyl sulfoxide: comparison of hydrogen-bond patterns and conformational behaviour, Carbohydr. Res. 230 (1) (1992) 1–13, https://doi.org/10.1016/s0008-6215(00)90509-3.
[54] S. Kalyanam, R.D. Yapp, M.F. Insana, Poro-viscoelastic behavior of gelatin hydrogels under compression-implications for bioelasticity imaging, J. Biomech. Eng. 131 (8) (2009), 081005, https://doi.org/10.1115/1.3127250.
[55] D.B. Deegan, C. Zimmerman, A. Skardal, A. Atala, T.D. Shupe, Stiffness of hyaluronic acid gels containing liver extracellular matrix supports human hepatocyte function and alters cell morphology, J. Mech. Behav. Biomed. Mater. 55 (2015) 87–103, https://doi.org/10.1016/j.jmbbm.2015.10.016.
[56] Y. Zhang, J. Lu, Z. Li, D. Zhu, X. Yu, L. Li, Enhanced cellular functions of hepatocytes in the hyaluronate-alginate-chitosan microcapsules, Int J Artif Organs 44 (5) (2021) 340–349, https://doi.org/10.1177/0391398820959345.
[57] S.S. Desai, J.C. Tung, V.X. Zhou, et al., Physiological ranges of matrix rigidity modulate primary mouse hepatocyte function in part through hepatocyte nuclear factor 4 alpha, Hepatology 64 (1) (2016) 261–275, https://doi.org/10.1002/hep.28450.
[58] W.C. Yeh, P.C. Li, Y.M. Jeng, et al., Elastic modulus measurements of human liver and correlation with pathology, Ultrasound Med. Biol. 28 (4) (2002) 467–474, https://doi.org/10.1016/s0301-5629(02)00489-1.
[59] K.J. De France, F. Xu, T. Hoare, Structured macroporous hydrogels: progress, challenges, and opportunities, Adv Healthc Mater 7 (1) (2018), https://doi.org/10.1002/adhm.201700927.
[60] M. Modriansky, J. Ulrichova, P. Bachleda, et al., Human hepatocyte–a model for toxicological studies. Functional and biochemical characterization, Gen. Physiol. Biophys. 19 (2) (2000) 223–235.
[61] T. Soga, R. Baran, M. Suematsu, et al., Differential metabolomics reveals ophthalmic acid as an oxidative stress biomarker indicating hepatic glutathione consumption, J. Biol. Chem. 281 (24) (2006) 16768–16776, https://doi.org/10.1074/jbc.M601876200.
[62] J.A. Lawson, A. Farhood, R.D. Hopper, M.L. Bajt, H. Jaeschke, The hepatic inflammatory response after acetaminophen overdose: role of neutrophils, Toxicol. Sci. 54 (2) (2000) 509–516, https://doi.org/10.1093/toxsci/54.2.509.
[63] M. Rezaeeyazdi, T. Colombani, A. Memic, S.A. Bencherif, Injectable hyaluronic acid-co-gelatin Cryogels for tissue-engineering applications, Materials (Basel) 11 (8) (2018), https://doi.org/10.3390/ma11081374.
[64] C. Gao, Y. Yang, Y. Zhang, M. Qian, J. Yang, HGF gene delivering alginate/Galactosylated chitosan sponge scaffold for three-dimensional Coculture of hepatocytes/3T3 cells, DNA Cell Biol. 39 (3) (2020) 451–458, https://doi.org/10.1089/dna.2019.5136.
[65] C.L. German, S.V. Madihally, Type of endothelial cells affects HepaRG cell acetaminophen metabolism in both 2D and 3D porous scaffold cultures, J. Appl. Toxicol. 39 (3) (2019) 461–472, https://doi.org/10.1002/jat.3737.
[66] C.S. Ranucci, A. Kumar, S.P. Batra, P.V. Moghe, Control of hepatocyte function on collagen foams: sizing matrix pores toward selective induction of 2-D and 3-D cellular morphogenesis, Biomaterials 21 (8) (2000) 783–793, https://doi.org/10.1016/s0142-9612(99)00238-0.
[67] J. Fan, Y. Shang, Y. Yuan, J. Yang, Preparation and characterization of chitosan/galactosylated hyaluronic acid scaffolds for primary hepatocytes culture, J Mater Sci Mater Med 21 (1) (2010) 319–327, https://doi.org/10.1007/s10856-009-3833-y.
[68] Z. Feng, W. Ning Chen, P. Vee Sin Lee, K. Liao, V. Chan, The influence of GFP-actin expression on the adhesion dynamics of HepG2 cells on a model extracellular matrix, Biomaterials 26 (26) (2005) 5348–5358, https://doi.org/10.1016/j.biomaterials.2005.01.069.
[69] S. Cannito, V. Bincoletto, C. Turato, et al., Hyaluronated and PEGylated liposomes as a potential drug-delivery strategy to specifically target liver cancer and inflammatory cells, Molecules 27 (3) (2022), https://doi.org/10.3390/molecules27031062.
[70] A. Mazzocchi, K.M. Yoo, K.G. Nairon, et al., Exploiting maleimide-functionalized hyaluronan hydrogels to test cellular responses to physical and biochemical stimuli, Biomed. Mater. 17 (2) (2022), https://doi.org/10.1088/1748-605X/ac45eb.
[71] C. Chen, A. Soto-Gutierrez, P.M. Baptista, B. Spee, Biotechnology challenges to in vitro maturation of hepatic stem cells, Gastroenterology 154 (5) (2018) 1258–1272, https://doi.org/10.1053/j.gastro.2018.01.066.
[72] P. Starkey Lewis, L. Campana, N. Aleksieva, et al., Alternatively activated macrophages promote resolution of necrosis following acute liver injury, J. Hepatol. 73 (2) (2020) 349–360, https://doi.org/10.1016/j.jhep.2020.02.031.
[73] C. Le Guilcher, G. Merlen, A. Dellaquila, et al., Engineered human liver based on pullulan-dextran hydrogel promotes mice survival after liver failure, Mater Today Bio 19 (2023), 100554, https://doi.org/10.1016/j.mtbio.2023.100554.
[74] J. Zhang, Y. Xu, C. Zhuo, et al., Highly efficient fabrication of functional hepatocyte spheroids by a magnetic system for the rescue of acute liver failure, Biomaterials 294 (2023), 122014, https://doi.org/10.1016/j.biomaterials.2023.122014.
[75] A. Ramachandran, H. Jaeschke, Mechanisms of acetaminophen hepatotoxicity and their translation to the human pathophysiology, J Clin Transl Res 3 (Suppl. 1) (2017) 157–169, https://doi.org/10.18053/jctres.03.2017S1.002.
[76] G. Kaur, E.M. Leslie, H. Tillman, et al., Detection of ophthalmic acid in serum from acetaminophen-induced acute liver failure patients is more frequent in non-survivors, PLoS One 10 (9) (2015), e0139299, https://doi.org/10.1371/journal.pone.0139299.
[77] S. Gupta, P. Rajvanshi, R. Sokhi, et al., Entry and integration of transplanted hepatocytes in rat liver plates occur by disruption of hepatic sinusoidal endothelium, Hepatology 29 (2) (1999) 509–519, https://doi.org/10.1002/hep.510290213.
[78] T. Ma, X.J. Gao, H. Dong, H.M. He, X.D. Cao, High-throughput generation of hyaluronic acid microgels via microfluidics-assisted enzymatic crosslinking and/or Diels-Alder click chemistry for cell encapsulation and delivery, Appl. Mater. Today 9 (2017) 49–59, https://doi.org/10.1016/j.apmt.2017.01.007.
[79] T. Kamperman, S. Henke, B. Zoetebier, et al., Nanoemulsion-induced enzymatic crosslinking of tyramine-functionalized polymer droplets, J. Mater. Chem. B 5 (25) (2017) 4835–4844, https://doi.org/10.1039/c7tb00686a.
[80] S.J. Forbes, S. Gupta, A. Dhawan, Cell therapy for liver disease: from liver transplantation to cell factory, J. Hepatol. 62 (1 Suppl) (2015), https://doi.org/10.1016/j.jhep.2015.02.040. S157-69 S0168-8278(15)00156-7 [pii].
[81] L. Tolosa, J. Caron, Z. Hannoun, et al., Transplantation of hESC-derived hepatocytes protects mice from liver injury, Stem Cell Res Ther 6 (2015) 246, https://doi.org/10.1186/s13287-015-0227-6.
[82] E. Zigmond, S. Samia-Grinberg, M. Pasmanik-Chor, et al., Infiltrating monocyte-derived macrophages and resident kupffer cells display different ontogeny and functions in acute liver injury, J. Immunol. 193 (1) (2014) 344–353, https://doi.org/10.4049/jimmunol.1400574.
[83] B.S. Ding, D.J. Nolan, J.M. Butler, et al., Inductive angiocrine signals from sinusoidal endothelium are required for liver regeneration, Nature 468 (7321) (2010) 310–315, https://doi.org/10.1038/nature09493.
[84] T. Takebe, K. Sekine, M. Enomura, et al., Vascularized and functional human liver from an iPSC-derived organ bud transplant, Nature 499 (7459) (2013) 481–484, https://doi.org/10.1038/nature12271.